A Sea Floor Gravity Survey of the Sleipner Field to Monitor CO_2 Migration

Technical Progress Report

Reporting Period: 9/19/04 - 3/18/05

PI: Mark Zumberge

Principal Authors:
Scott Nooner
Mark A. Zumberge
Scripps Institution of Oceanography
9500 Gilman Drive
La Jolla, CA 92093-0225

Report Issued: 7/11/05

DOE Award Number: DE-FC26-02NT41587

DISCLAIMER

Abstract

Since 1996, excess CO_2 from the Sleipner natural gas field has been sequestered and injected underground into a porous saline aquifer 1000 m below the seafloor. In 2002, we carried out a high precision micro-gravity survey on the seafloor in order to monitor the injected CO_2. A repeatability of 5 μGal in the station averages was observed. This is considerably better than pre-survey expectations. These data will serve as the baseline for time-lapse gravity monitoring of the Sleipner CO_2 injection site. A repeat survey has been scheduled for the summer of 2005. This report covers 9/19/04 to 3/18/05. During this time, gravity and pressure modeling were completed and work graduate student Scott Nooner began writing his Ph.D. dissertation, of which this work is a the major part. Improvements to the gravimeters are also underway that will hopefully increase the measurement precision.

Table of Contents

Executive Summary

This document is a report detailing the continuing work that has been done under DOE Award DE-FC26-02NT41587, which started September 19, 2002. This work, the quantification of gravity change associated with the sequestration of CO_2 at the Sleipner gas field in the North Sea, is a collaborative research effort between US scientists and members of the SACS (Saline Aquifer CO_2 Storage) consortium. At this site, about 1 Mton of excess CO_2 is extracted from the natural gas each year and then injected into a porous saline aquifer (the Utsira formation) at about 1000 m below the seafloor (Baklid et al., 1996). Because CO_2 has never been compressed and injected underground for sequestration before, it is important to monitor what happens as time passes.

As this gas is injected into the storage reservoir, the overall density of the rock and pore space decreases. This decrease in density has an effect on the local strength of gravity. By monitoring how the local gravity field changes with time, we can assess the extent to which the gas is successfully contained and we can put constraints on the density of CO_2 within the reservoir.

Near predicted reservoir temperature and pressure conditions, CO_2 goes through a critical phase transition in which the density changes from 200 kg/m^3 to over 700 kg/m^3 over a short range of temperature [Span and Wagner, 1996]. Thus, a slightly higher temperature could result in a much lower CO_2 density. Therefore, a feasibility study for monitoring the CO_2 bubble expansion by time-lapse gravity measurements was done by Williamson et al., (2001). They computed the gravity signals from both a high and a low-density model. The low-density model (350 kg/m^3) shows a peak anomaly of -34 μGal, while the high-density model (700 kg/m^3) shows a peak anomaly of -7 μGal after 2.268 MT of CO_2 was injected (slightly over two years). If significant amounts of CO_2 penetrate above the top seal, density will be further reduced and the gas will be closer to the observation points, causing gravity changes that could well exceed 100 μGal, making gravity an effective tool for measuring catastrophic leaks.

Gravity was measured on the seafloor above the Sleipner CO_2 injection site from the 15th to the 21st of August 2002, on top of 30 concrete benchmarks, which were permanently deployed on the seafloor. The area spans about 7 km E-W and 3 km N-S. In relative gravity surveys, the uncertainty is given by the repeatability of the measurements, thus each benchmark was visited at least three times. Repeatability for a single gravimeter is estimated to be 4.3 μGal. These data will serve as a baseline for future monitoring of the CO_2 bubble. For time-lapse measurements, there is additional uncertainty associated with the reference benchmark, determined from stations outside the CO_2 area, of about 1-2 μGal. Therefore, the final detection threshold for time-lapse changes is about 5 μGal. This is considerably better than the pre-survey expectations of 10 μGal, and increases the likelihood of detecting time-lapse changes. Single observation relative depth estimates have a repeatability of 0.5 cm, which also makes monitoring of small vertical seafloor movements in the area possible.

Based on the original survey alone, a limited amount of information about the injected CO_2 can be obtained. A future repeat gravity survey is the only way to provide an independent and reliable means to quantify the CO_2. We expect that in a second

survey, any gravity change will be due to the changing CO_2 volume, not the presumed stable geologic setting. A repeat survey is scheduled for the summer of 2005.

We developed our own software to do the gravity modeling, since no commercial software could do what we needed. Using this software, we have been able to place bounds on the expected time-lapse gravity signal, which will allow us to constrain the CO_2 density within the reservoir. For low density CO_2, we expect to see a gravity change of 7-9 μGal/year and for high density CO_2 we expect to see a gravity change of 2-3 μGal/year. For a 3-year span between surveys (2002-2005), this means a maximum gravity change between 27 μGal or 9 μGal, depending on the CO_2 density within the reservoir. By calculating the seismic velocity pushdown (time delay in the two-way vertical travel time), some constraints can be placed on the geometry of the intra-reservoir CO_2. Deformation of the seafloor could also provide information about the stored CO_2. Mechanical modeling of the reservoir indicate that the maximum possible uplift expected is ~0.16 cm/yr, or about 0.5 cm over 3 years. However, the depth resolution of our seawater pressure measurements (obtained along with gravity) is about 0.5 cm, based on the repeatability of the pressure measurements in the first survey. Therefore, we don't expect to see a seafloor deformation signal in within the first 3 years.

We have also begun preparation for the first repeat survey in the summer of 2005. We are have been making improvements to the gravimeters in hope of increasing the measurements precision.

Experimental

In microgravity reservoir monitoring surveys on land [e.g. Allis and Hunt, 1986; San Andres and Pedersen, 1993] accuracies of 10 μGal or better have been achieved by careful use of standard gravimeters. However, ship-borne measurements have uncertainties of several hundreds of μGal, making offshore gravity monitoring difficult. A new seafloor gravimeter (ROVDOG for ROV deployed Deep Ocean Gravimeter) has been developed by Scripps Institution of Oceanography and Statoil [Sasagawa et al., 2003; Eiken et al., 2000]. The collection of seafloor gravity data is desirable because the signal-to-noise ratio is significantly better than that of sea surface data. The primary benefit, however, is that the ROVDOG is placed directly on the seafloor and is connected to the deployment vehicle via only a loose tether, eliminating all accelerations caused by ship and vehicle. Also, by deploying the instrument with an ROV onto seafloor benchmarks, positioning uncertainties related to site reoccupation are virtually eliminated.

Water pressure is also measured in our instrument package for high-accuracy relative depth measurements. Separate stationary reference pressure gauges are also deployed for the survey period to record tidal signals, which need to be taken out of the relative pressure records.

The primary sensor in the ROVDOG instrument is a modified Scintrex CG-3M gravimeter mounted in a compact gimbal platform for leveling and enclosed, along with a Paroscientific 31K pressure gauge, in a watertight pressure case. Three pressure cases were mounted on a frame (Figure 1). The instrument is described in more detail in Sasagawa et al. [2003].

Figure 1: ROVDOG II

Benchmarks were deployed in a 10-hour period just before surveying, on August 16, 2002. 20 of the benchmarks were placed in a 7.3 km long WNW-ESE profile across the injection point (Figure 2). The distance between stations increases from about 300 m near the injection point up to 500 m towards the ends. Another 10 locations span the orthogonal dimension and cover the extent of the CO_2 accumulation in 2002.

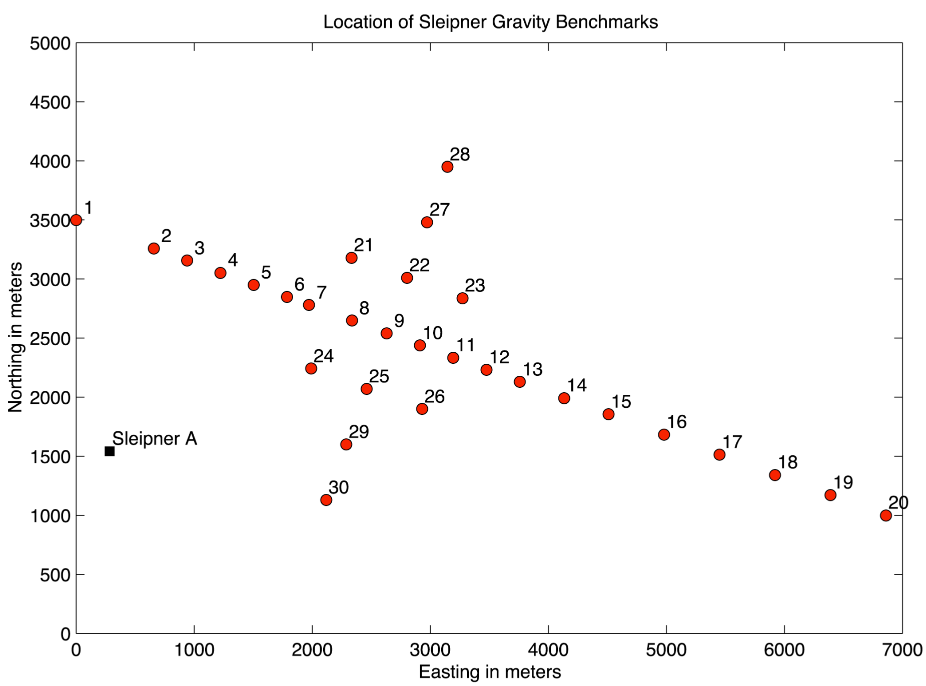

Figure 2. Sleipner gravity benchmark locations are shown in red.

The gravity data were analyzed in collaboration with Ola Eiken and Torkjell Stenvold from Statoil (as discussed in previous technical reports). We found the repeatability of the meters to be about 2.5 μGal, making the observable signal size from a time-lapse measurement about 5 μGal.

After investigating and testing the commercial software, we realized that we needed to write our own code to do the 3-D gravity modeling. The primary reasons behind this are 1. We needed to calculate gravity from an arbitrary shape, 2. We needed to be able to compute the gravity from a volumetric grid (from the SINTEF reservoir simulation models), and 3. We needed to vary the density of the arbitrarily shaped body both horizontally and vertically. This led us to develop code to construct mass bodies from either a collection of cuboids or point masses.

Results

Gravity Modeling

We concluded our study of the expected gravity signal at Sleipner. The time-lapse gravity signal was estimated from two types of models. The first type uses the seismically imaged CO_2 horizons and velocity pushdown for 1999 and 2001. The second type of model was based on reservoir simulation models done by SINTEF. The seismic data provide the only way, currently, to measure *in situ* CO_2 mass at Sleipner. However, there are discrepancies between the reservoir characteristics that seem to be required by the seismic data and the physics of the reservoir flow models. If geologic sequestration of CO_2 is to become a widely used method for carbon capture, the behavior of CO_2 within reservoirs such as the Utsira formation must be well understood. Part of this is simply in understanding the physical characteristics, such as temperature and density, of CO_2 within the reservoir. The primary goal of this study is to put constraints on CO_2 density and temperature within the reservoir. A secondary goal is to provide an independent technique for quantifying the CO_2 mass within the reservoir.

The seismic data from 1999 and 2001 were used to build models of injected CO_2 for two scenarios. The first is for an average CO_2 density within the reservoir of 700 kg/m^3, and the second is for an average CO_2 density of 550 kg/m^3. These correspond to low reservoir temperature (35 ºC) and high reservoir temperature (45 ºC) scenarios, respectively. These models contain supercritical CO_2 in two distinct parts. The first is CO_2 residing in thin high saturation layers, which have ponded beneath thin inter-reservoir shale layers. These can be seen as layers of increased reflectivity in the time-lapse seismic data. The second volume of CO_2 is a low saturation diffuse volume occupying the space between the high saturation layers. This diffuse volume of CO_2 does not cause increased reflectivity, but its existence is indicated by a larger observed seismic pushdown than is expected from the high saturation layers alone. The amount of diffuse CO_2 is uncertain, and depends upon the CO_2 density and upon the details of its distribution. The modeling approach is similar to *Chadwick et al.* [2002] and is summarized below:

1. Calculate a thin-layer model for the high saturation CO_2 layers.
2. Calculate the gravity from this model.

3. Calculate the velocity pushdown from this model.
4. Subtract the calculated pushdown from the observed pushdown to obtain the residual pushdown.
5. Use the residual pushdown to calculate the average vertical saturation for the diffuse volume.
6. Calculate the gravity from the diffuse CO_2 model and combine with the gravity calculated from the layers.
7. Compute the total mass and volume of CO_2 in the combined model.

The reflection amplitude of the seismic horizons was provided as xyz data by Ola Eiken and the SACS consortium. To work with the data, each horizon was first converted into to a regularly spaced grid. For the thin layer model, the reflection amplitudes of the horizons were then linearly related to layer thickness with the maximum reflection amplitude being set equal to 8 m, corresponding to the tuning thickness of the seismic wavelet [*Arts et al.*, 2002b]. The mass of CO_2 at each grid point can be calculated by

$$m = \rho_{CO_2} S_{CO_2} \phi \cdot dx \cdot dy \cdot dz , \qquad 1$$

where *dx* and *dy* are the grid spacings, *dz* is the layer thickness, ρ_{CO_2} is the density of CO_2, ϕ is the porosity, and S_{CO_2} is the saturation of CO_2. The only unknown is the saturation of CO_2, which varies with height, *h*, in each CO_2 layer due to capillary pressure, p_c, between the formation brine and injected CO_2. This relationship in SI units was determined by centrifuge experiments on core material from the Utsira Sand [*Chadwick et al.*, 2002; *Chadwick et al.*, 2004]:

$$p_c = \Delta \rho g h = 810.35(1 - S_{CO_2})^{-0.948} . \qquad 2$$

In the above equation $\Delta\rho$ is the density difference between water and CO_2 within the reservoir. Figure 3 shows the CO_2 saturation as a function of height, *h*, and the average layer saturation as a function of layer thickness, *dz*. The average saturation was obtained by solving equation 2 for S_{CO_2} and substituting into the following:

$$S_{ave} = \frac{1}{dz} \int_0^{dz} S_{CO_2} dh . \qquad 3$$

The mass of CO_2 at each grid point can then be calculated from equation 1 using the layer thickness, *dz*, and the average CO_2 saturation, S_{ave}.

The thin layer mass calculated for the low-density (high reservoir temperature) case is 0.853 MT in 1999 (36.3% of the injected amount) and 1.5 MT in 2001 (34.0% of the injected amount). For the high-density (high reservoir temperature) case, the mass is 1.53 MT in 1999 (65.1% of the injected amount) and 2.69 MT in 2001 (61.2% of the injected amount). Uncertainty in these figures comes from uncertainty in the interpretation of the seismic horizons, errors in the simple amplitude to thickness conversion, and reflectivity attenuation in the deeper parts of the plume which are difficult to quantify [*Chadwick et al.*, 2002]. The 3-D gravity modeling code was then used to compute the gravity signal from the thin CO_2 layers.

The seismic pushdown from the layers is the difference in two-way travel-time (twtt) caused by the presence of the CO_2. This can be found from the change in seismic velocity, which can be found using Gassmann's relationships. The velocity changes rapidly for low saturations, but for saturations larger than about 0.2 it changes very little, particularly for homogeneous distributions. The pushdown for each density scenario for both years was then calculated and subtracted from the total observed pushdown to give the residual pushdown (Figure 4). This residual pushdown is caused by CO_2 that is not present in the thin layers, and requires the presence of additional CO_2 within the reservoir.

Using only the thin, high saturation CO_2 layers does not account for either the total injected mass or the total observed pushdown for either density scenario. The residual pushdown is concentrated in the central region of the plume, near the central chimney, consistent with the presence of diffuse CO_2 in the axial region. *Arts et al.* [2002b] plotted seismic amplitudes against velocity pushdown in various parts of the plume. Outer parts of the plume obey the thin-bed tuning relationship, whereas in axial parts of the plume, pushdown values are much higher for a given seismic amplitude. This indicates the presence of lower saturation CO_2. *Chadwick et al.* [2004] showed that the ratio of velocity pushdown to plume reflectivity is much higher in the axial parts of the plume than at its edges, also consistent with the presence of diffuse CO_2.

The next step, then, is to use the residual pushdown to estimate the saturation and mass of the diffuse CO_2 volume using the velocity versus saturation curves shown in Figure 2.6. The pushdown, ΔT, is defined as follows:

$$\Delta T = 2\left(\frac{1}{V_{S_{CO_2}}} - \frac{1}{V}\right)dz, \qquad 4$$

where $V_{S_{CO_2}}$ is the seismic velocity with CO_2 present, V is the velocity without the presence of CO_2, and dz is the vertical thickness of the CO_2. Equation 2.5.8 can be rearranged to solve for $V_{S_{CO_2}}$ from the pushdown:

$$V_{S_{CO_2}} = \left(\frac{\Delta T}{2dz} + \frac{1}{V}\right)^{-1}. \qquad 5$$

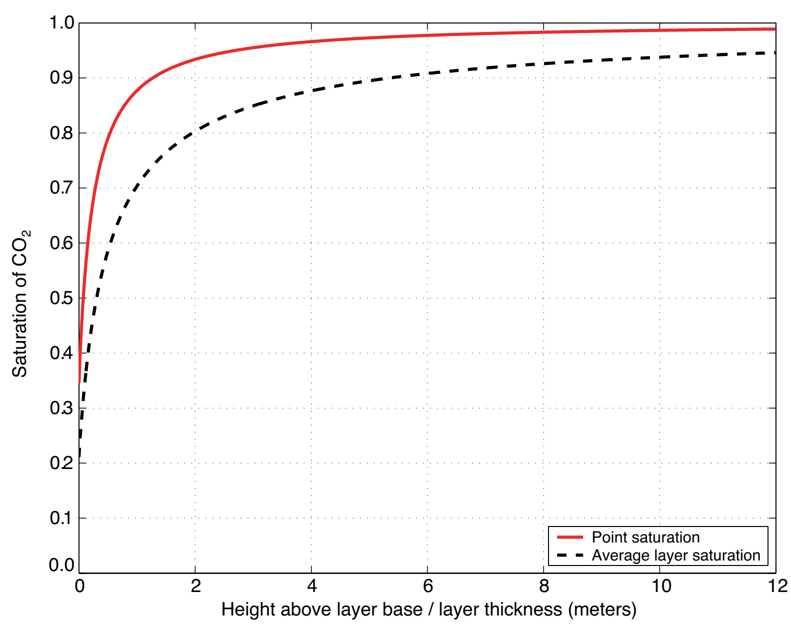

Figure 3 Plot showing both point saturation as a function of height above layer base (solid curve) and average layer saturation as a function of layer thickness (dashed curve). Both are calculated from the capillary pressure – saturation relationship given in equation 2.

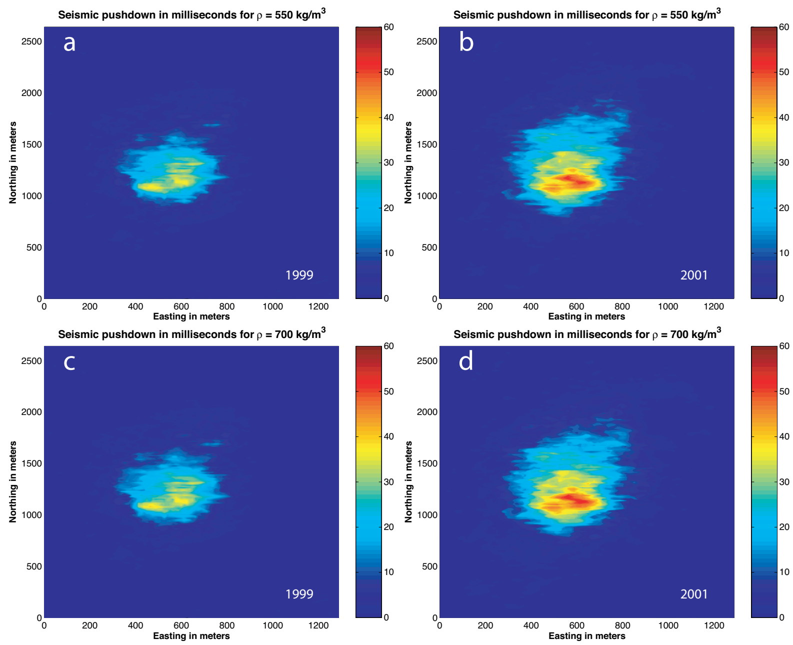

Figure 4 Residual pushdown in milliseconds is calculated by subtracting the theoretical pushdown of the CO_2 horizons from the observed pushdown. Pushdown for a.) 1999 low-density model, b.) 2001 low-density model, c.) 1999 high-density model, and d.) 2001 high-density model. There is very little difference in the residual pushdown for the two density cases.

To solve for $V_{S_{CO_2}}$ from equation 5, an estimate must be made for the vertical thickness, *dz*. This introduces a non-unique element into the problem. An infinite number of distributions of diffuse CO_2 can be made to satisfy the residual pushdown. To estimate *dz* in a meaningful way, we first defined a volume enclosing the diffuse CO_2. A reasonable assumption is that the diffuse CO_2 resides near the higher saturation volumes (the thin layers and the chimney), but is not found some characteristic distance away, which we chose to be 25 m. This value is two times the grid spacing and is close to the average distance between shale layers, which is 30 m. Therefore, an algorithm stepped through the seismic horizons and every grid point within the characteristic distance from a high saturation grid point was included in the volume. Points that were within 1.75 m of a seismic horizon (corresponding to the average CO_2 layer thickness) were excluded from the volume. This created the gridded 3-D volume enclosing the horizons shown in Figure 5. The vertical thickness, *dz,* was then calculated by summing the number of grid points in each vertical column included in the volume and multiplying each resulting number by the vertical grid spacing (12.5 m). The residual pushdown, ΔT, and the vertical thickness, *dz*, were then used together to solve for the average velocity, $V_{S_{CO_2}}$, through the diffuse CO_2.

A density of CO_2 was then chosen and $V_{S_{CO_2}}$ was then used to determine an average CO_2 value at each point using the appropriate velocity versus saturation curve . Because the seismic velocity changes very little for saturation values greater than 0.2, small errors in the calculation of $V_{S_{CO_2}}$ can lead to large uncertainty in the resulting saturation estimate. These uncertainties are difficult to quantify. Nevertheless, the resulting model for the diffuse volume is a CO_2 distribution in which the CO_2 saturation varies laterally, but is constant vertically. This is obviously not likely to be the real distribution, but it probably provides a good estimate of the gravity field, since the vertical variation will have little effect on gravity.

The mass in the diffuse volume can then be calculated from equation 1. For the low-density case, the diffuse CO_2 contains 0.15 MT for 1999 and 0.28 MT for 2001. Adding this to the thin layer mass gives 1.43 MT for 1999 (60.94 % of the known injected mass) and 2.53 MT for 2001 (59.36 % of the known injected mass).
For the high-density case, the diffuse CO_2 contains 0.384 MT for 1999 and 0.752 MT for 2001. Adding this to the thin layer mass gives 1.94 MT for 1999 (82.75 % of the known injected mass) and 3.49 MT for 2001 (81.85 % of the known injected mass).

The contribution of the diffuse volume to the gravity signal is then calculated with our 3-D code. Combining the layer contribution with the diffuse volume contribution indicates that the high-density scenario would cause maximum change of about 2.7 μGal/year, while the low-density scenario would cause a maximum change of about 3.5 μGal/year (Figure 6).

Reservoir simulation models provide insight into the behavior of the injected CO_2. However, these flow models are highly dependent on reservoir characteristics such as temperature. Calculating the expected gravity change on the seafloor from reservoir flow models provides a way, independent of seismic data, to use time-lapse gravity to put constraints on the density (hence temperature) of CO_2 within the Utsira formation. Reservoir modeling at Sleipner has been done by the Norwegian company SINTEF, Scandinavia's largest independent research organization (http://www.sintef.no). SINTEF produced 3-D saturation grids from CO_2 flow simulations, which were created using the commercial reservoir modeling software Eclipse. The models were for a three-dimensional volume with a permeability of 2 darcy and a porosity of 0.38, cut laterally by five impermeable layers (representing shale). The shape of these layers was guided by the geometry of the seismically imaged CO_2 horizons. The boundaries of the model volume were kept at a constant pressure, simulating an infinite reservoir [*Sjur Mo*, personal communication, 2003]. Two types of simulation models were examined. The first type, model I, has a central chimney and horizontal CO_2 layers like the seismic model; however, it has no low saturation volume (Figure 2.23). The engineers at SINTEF have not been able to produce a CO_2 flow scenario resulting in a low saturation volume as suggested by the seismic pushdown. Therefore, a second model was examined, model II, composed of several micro-chimneys, which, if small enough, might look like a diffuse volume of CO_2 to seismic energy (Figure 2.23). This was created by randomly distributing 640 holes within the impermeable shale layers. Each hole has an increased permeability. Simulations for model II spanning 20 years were computed by SINTEF for average reservoir temperatures of both 37 ºC and 45 ºC, corresponding to CO_2 densities of ρ_{co_2} = 750 kg/m^3 and ρ_{co_2} = 550 kg/m^3 (call them models IIa and IIb, respectively). The CO_2 injection rate plotted against year for the simulations is shown in Figure 7. The reservoir simulations also predict the amount of CO_2 that dissolves in the brine over time (Figure 7). Therefore, the mass contributing to the gravity signal will be the total injected amount of CO_2 minus the dissolved CO_2.

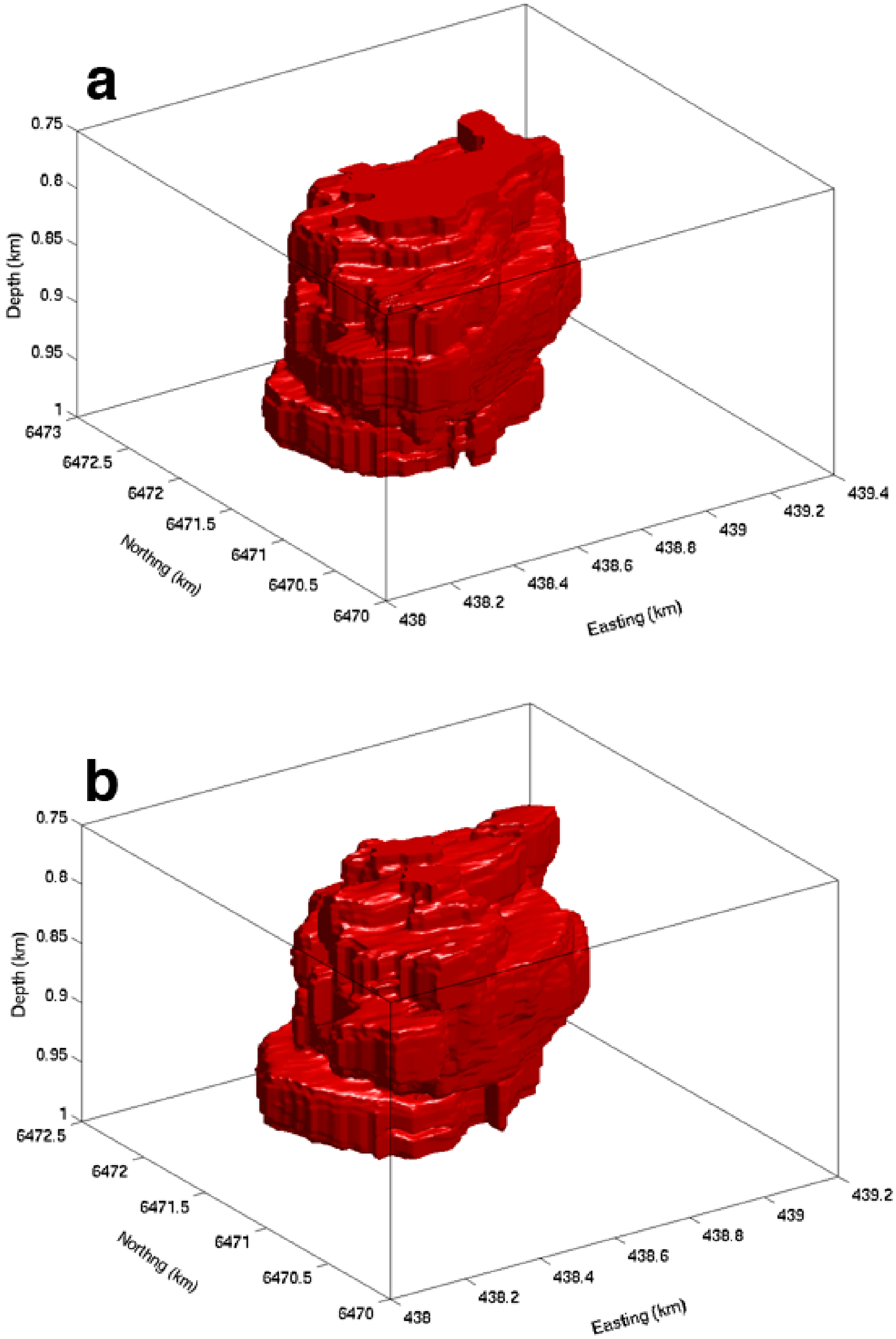

Figure 5 The volume enclosing the diffuse, low-saturation CO_2 in the models based on the time-lapse 3-D seismic data for a.) 1999 and b.) 2001.

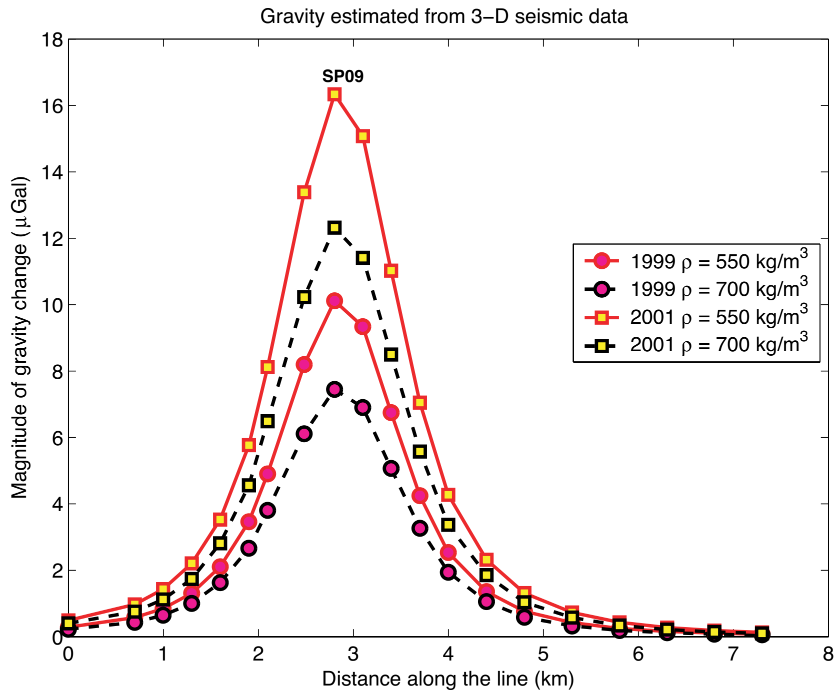

Figure 6 This plot shows the magnitude of the gravity change calculated from the both the 1999 and 2001 seismic data. The points along the line represent the seafloor benchmarks along the NW-SE line shown in Figure 2.10 (benchmark SP09 is indicated above). Calculations were made using two different densities, as indicated in the figure.

The output of each flow model is a volumetric CO_2 saturation grid containing 428,400 grid points ($70 \times 85 \times 72$). The thickness of the grid blocks varies from 15.2 m to 0.2 m with depth, as the grid is refined below the shale layers (where most of the CO_2 resides). The horizontal grid spacing is constant at $dx = 34.4$ m and $dy = 36.1$ m.

The results of these reservoir models were used in the current study to calculate the expected seafloor gravity caused by the CO_2 injection. Saturation, S_{CO_2}, was converted to a change in mass at each grid point using a reservoir porosity of $\phi = 0.37$, a shale fraction of $v_{sh} = 0.01$, a cell volume of $V = dx \cdot dy \cdot dz$, and a CO_2 density ρ_{CO_2} dependent on the flow model:

$$\Delta M = \Delta \rho V \phi (1 - v_{sh}) S_{CO_2}, \qquad 6$$

where $\Delta M = M_{CO_2} - M_{H_2O}$ and $\Delta \rho = \rho_{CO_2} - \rho_{H_2O}$. Gravity was then calculated using either equation 2.5.2 or 2.5.3 by treating each mass ΔM as a point mass. Later, a new computer (Power Mac G5, dual 2.5 GHz) allowed us to recalculate gravity for each simulation model, treating each grid block as a cuboid. The results are indistinguishable from the point mass approximation.

The time varying gravity spanning 1996 to 2002 computed on the seafloor benchmarks from model I is shown in Figure 8, indicating a maximum gravity change of about 2.2 μGal/year. Model IIa (Figure 8) spans the years 1996 to 2016 and predicts a maximum change of about 2.4 μGal/year. A comparison of these two models is shown in Figure 9 for 2001. Interestingly, the results are almost identical, in spite of the fact that

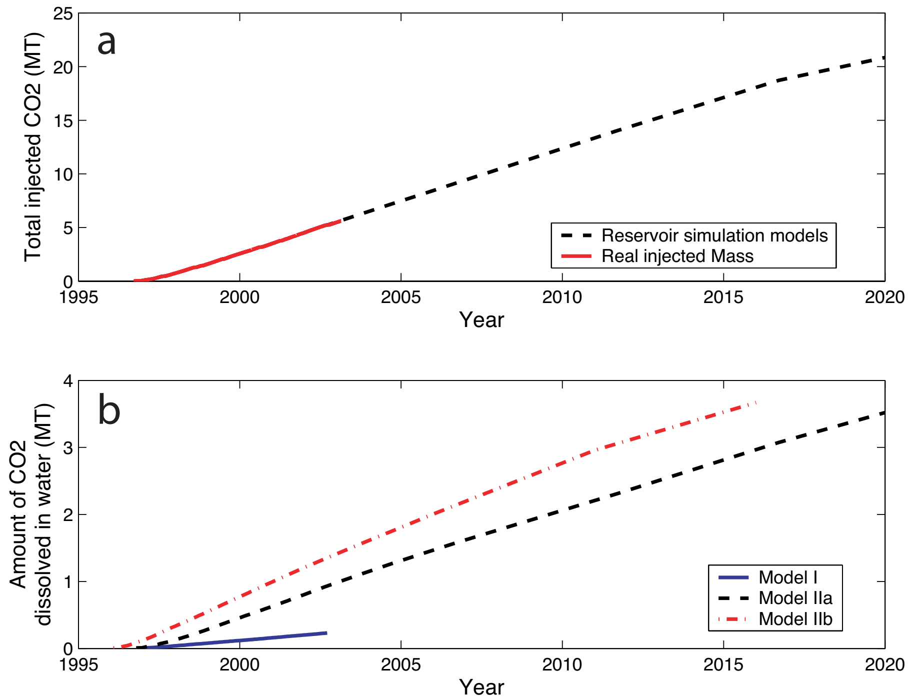

Figure 7 a.) The total injected CO_2 mass in MT is plotted in red. The injected mass used in the reservoir simulation models follows the real injected mass until 2004 and continues along the black dashed line. b.) The expected amount of dissolved CO_2 in MT is shown for the different reservoir simulation models. Dissolution rates are approximately 4% for Model I, 17% for Model IIa, and 23% for Model IIb.

the models have dissolution rates for CO_2 into the aquifer brine. Model I is composed of a horizontal layers central chimney, while model IIa is composed of horizontal layers andmultiple vertical chimneys. This means that model IIa has a larger surface area of CO_2 in contact with the brine, allowing more dissolution to take place (~4.5 % in model I and ~17.5% in model IIa, Figure 7b). Therefore, for the same amount of injected mass, model I has more undissolved CO_2.

Figure 8c shows the time varying gravity for model IIb, which predicts a maximum gravity change of 4.7 μGal/year. The higher temperature of model IIb causes the CO_2 density to decrease, creating a larger density difference between the CO_2 and formation water. The lower density CO_2 also occupies more volume within the reservoir, increasing surface area in contact with the brine. The dissolution into water in this case is more than 23% (Figure 7b). The lower density CO_2 is also more buoyant, which tends to increase the gravity driven vertical flow. Therefore, compared to model IIa, more mass in model IIb is located in the shallow layers. By the year 2011, 6% of the injected CO_2 is flowing out of the model boundaries. There is more than 20% outflow by 2016, so the results for this year are an underestimate.

It is interesting to calculate the theoretical pushdown for the three models using velocity versus saturation relations shown in Figure 2.6. The saturation in each grid cell is an average saturation value for the volume enclosed. The residual pushdown for the three models is shown in Figure 10. None fits the observed pushdown that well, most

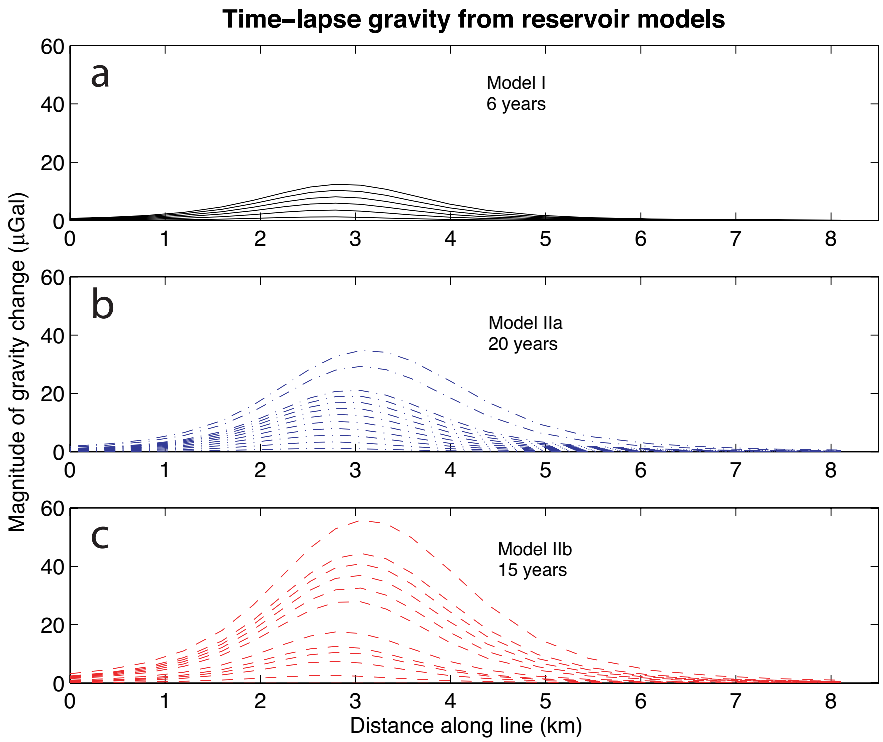

Figure 8 This figure shows the time varying gravity signals calculated from the reservoir simulation models. All models begin in 1996 and step forward by one year at a time. Model I stops in 2002 and Models IIa and IIb continue until 2006. These two models then jump to 2011 then Model IIa jumps to 2016. The results are shown above for a.) Model I, b.) Model IIa, and c.) Model IIb.

likely due to the lack of a low saturation diffuse volume of CO_2, which causes a large amount of pushdown for a relatively small mass. In fact, the pushdown from the reservoir simulation models show distinct points of large pushdown rather than the observed smooth distribution of pushdown. It seems possible that the seismically observed values contain some amount of horizontal averaging, although this possibility has not been reported.

We estimated the time-lapse gravity signal from two sets of models. In the first method, we took the seismically imaged CO_2 horizons for 1999 and 2001 and built a model based on them (Figure 3). The amplitudes of the horizons were linearly related to layer thickness with the maximum reflection amplitude being set equal to 8 m (Arts et al., 2002). This corresponds to the tuning thickness of the seismic wavelet (about 8 m in this case). The total mass of CO_2 was then calculated and compared to the known injected mass. The 'unaccounted for' mass was then put into a low saturation volume encompassing the horizons. The saturation of this 'diffuse' volume of CO_2 was estimated by calculating the This was done to take into account the requirement of the seismic pushdown effect to have a low saturation volume of CO_2. The seismic pushdown effect is caused by a decrease in seismic velocity through the CO_2 that has taken the place of water in the pore spaces within the reservoir. This decrease in velocity causes a corresponding increase in the travel-time of the seismic wave, causing a downward dip in the apparent horizontal layer depth (this can be seen in Figure 3).

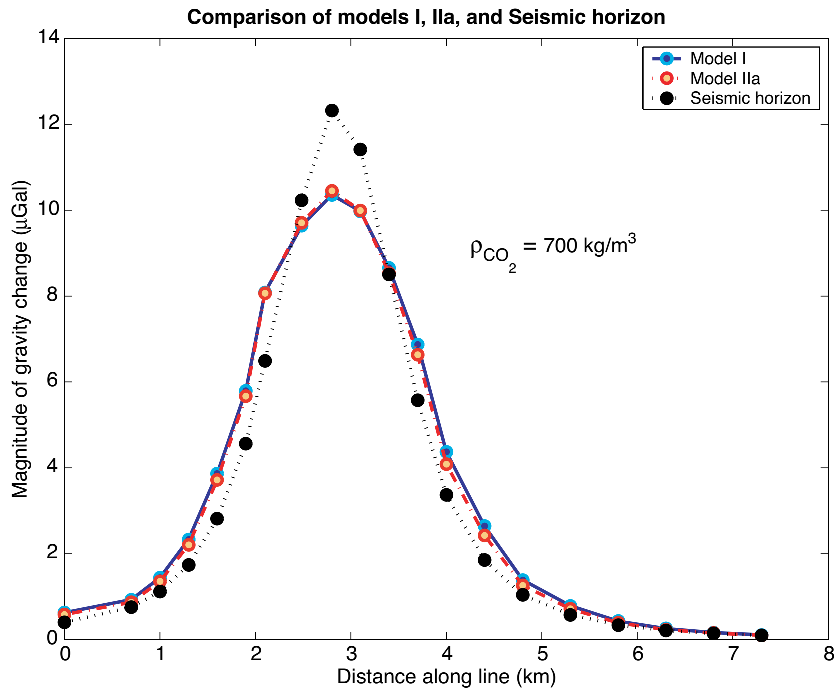

Figure 9 A comparison of the gravity calculated from models I and IIa, and from the seismic horizons in 2001. The injected mass is the same for both models (4.26 MT) and the density of CO_2 is 700 kg/m^3. The detailed geometry of the CO_2 distribution makes very little difference in the two reservoir models, but the seismic model differs in shape and maximum signal. However the maximum gravity change from 1999 is almost the same for all three models.

The time-lapse gravity signal was computed by comparing the results from the model based on the 2001 seismic data to the model based on the 1999 seismic data assuming a 1 MT/year injection rate. This was done for a high CO_2 density (ρ_{co_2} = 700 kg/m^3) scenario and a low CO_2 density (ρ_{co_2} = 350 kg/m^3) scenario. The results are that for the high-density scenario we expect to see a change of about 2 μGal/year and for the low-density scenario we expect to see a change of about 6 μGal/year (Figure 4).

The maximum gravity value predicted by the two types of models agree pretty well, indicating that the detailed geometry of the CO_2 bubble will not affect the estimated CO_2 density. The shape of the gravity curves (Figures 4 and 6) do reflect the geometry of the CO_2 bubble to some extent. However, this will probably be beyond the resolution of the technique for a three year time period.

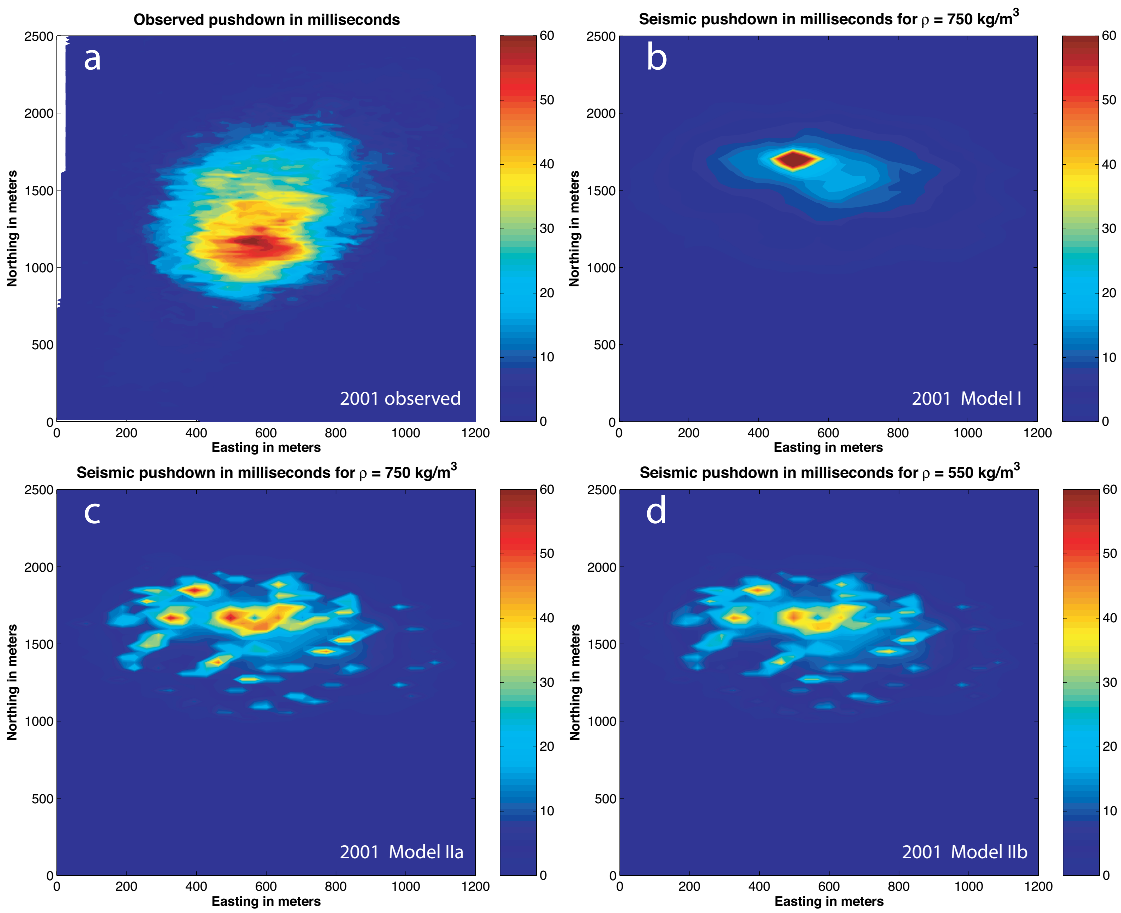

Figure 10 The pushdown estimated from the reservoir simulation models in comparison with the observed pushdown for 2001. a.) The observed pushdown, b.) Model I, c.) Model IIa, d.) Model IIb.

Discussion

By modeling the seismically imaged horizons in 1999 and 2001 as thin, high saturation layers and the residual seismic velocity pushdown as a low saturation non-reflective diffuse volume of CO_2, estimates for in situ CO_2 mass can be made. However, not all of the known injected amount of CO_2 is accounted for in these models. The high-density model, ρ_{co_2} = 750 kg/m^3, was able to account for almost 82 % of the known injected mass. From the reservoir simulation models, we expect about 17 % dissolution into aquifer water for the high-density case, suggesting that 99 % of the injected mass is contained. However, if the density of CO_2 in the aquifer is in the low-density state, with ρ_{co_2} = 550 kg/m^3, the seismic model accounts for only about 60 % of the injected mass, assuming a uniform distribution for the diffuse CO_2. Reservoir simulations indicate that just less than 23 % dissolution of CO_2 into water would occur, thus accounting for only about 83 % of the injected mass. This leaves 17 % of the mass missing in both 1999 and 2001.

For fluid filled rock, pore pressures can equilibrate over spatial scales of $L_c \approx \sqrt{kK_{fl}/f\eta}$, where f is the seismic frequency, k is the permeability, η is viscosity, and K_{fl} is the bulk modulus of the fluid [e.g., *Mavko and Mukerji*, 1998]. Heterogeneous saturations with length scales greater than L_c (referred to as patchy saturation) have wave-induced pore pressure gradients that cannot equilibrate, and patchy saturations always lead to higher seismic velocities than uniform saturations (saturations with length scales less than L_c). This means that for a given seismic pushdown, more mass is required by a patchy saturation than by a uniform saturation. Examples of two velocity versus average CO_2 saturation curves for patchy saturation models are shown in Figure 2.6. *Arts et al.* [2002b] showed that a patchy diffuse volume consisting of small patches of high saturation CO_2 could be constructed that would match both the observed pushdown and the injected mass for low-density CO_2. The reservoir simulation models seem to support the idea of heterogeneous saturation over a low saturation diffuse volume of CO_2 in that it is difficult to create large areas of uniform low saturation CO_2 from the physical flow models. This becomes obvious when comparing the predicted pushdown from the reservoir models to the observed pushdown (Figure 2.10). Heterogeneous saturations, however, can easily be caused by fingering of pore fluids and spatial variation in wettability, permeability, shaliness and etc. Some characteristic size and distribution of high saturation patches would have no observable reflectivity, but would cause a decrease in seismic velocity.

It is useful to revisit the low-density gravity model calculated from the seismic data in terms of a patchy CO_2 volume. It is a straightforward exercise to imagine putting the missing 17% back into the diffuse volume and redistributing the volume in such a way that the pushdown constraint is satisfied. From Table 1 it is apparent that (looking at the maximum gravity predicted) the diffuse volume of CO_2 accounts for 8.0 μGal/MT in 1999 and about 7.6 μGal/MT in 2001. Putting the missing 17 % of the injected CO_2 mass back into the model each year at the rates above adds 3.2 μGal to the maximum gravity in 1999 and 5.5 μGal in 2001. This means that the expected change in the maximum gravity increases from 3.3 μGal/yr to 4.5 μGal/yr.

Using this value means that the maximum gravity value predicted by the two types of models (seismic and reservoir simulation) have good agreement (Table 2.4). This indicates that the detailed geometry of the CO_2 bubble will not have a large effect on the observed gravity. This insensitivity to detailed flow geometry suggests that magnitude of the maximum time-lapse gravity signal we observe will be due to primarily CO_2 density, insuring that this technique will provide a robust estimate of CO_2 density. However, the gravity changes expected are small, meaning it may take some time to determine the CO_2 density. The difference between the two scenarios presented here (550 kg/m^3 and 750 kg/m^3) is about 2 μGal/yr, so after 5 or 6 years of measurements it should be possible to distinguish between the two with some confidence (our expected detection threshold is ~5 μGal). If the actual CO_2 density is between those two values, however, it will take more time to be able to make a confident statement about the density, perhaps up to 10 years or more. Finally, if the CO_2 density is lower than 550 kg/m^3, less time will be needed to determine the density.

The shape of the gravity curves (Figure 9) reflect the geometry of the CO_2 bubble to some extent, especially in the shape of the reservoir models versus the seismic model.

The wider peak in the reservoir models results from the CO_2 flow in the reservoir model going more east-west than the real flow. Over time, we may also be able to examine details of CO_2 flow using the shape of the gravity profile, but this will probably be beyond the resolution of the technique for a three year time period. Note that although the peak in the seismic model in Figure 9 is larger, the maximum change in gravity from 1999 is almost identical to the reservoir simulation models.

The first repeat gravity survey is scheduled for late summer of 2005, for a time span of three years. Therefore, we expect to see a maximum decrease in the observed gravity between 7 and 14 μGal, depending on the density of CO_2 within the reservoir (Table 1). Assuming the repeatability is similar to that of the first survey, it might just be possible to begin to distinguish between the two scenarios.

As a final exercise, we can examine an extreme case in which the reservoir temperature is warmer than 45 ºC. As the temperature increases, the average density of CO_2 within the reservoir decreases rapidly. Taking the average density of CO_2 as ρ_{co_2} = 350 kg/m^3 (caused by only a few degree increase), we can go through the procedure outlined in section 2.5.2 to calculate the expected gravity from the seismically imaged horizons. The pushdown can be estimated using the velocity versus saturation from the 45 ºC curve shown in Figure 2.6. This is obviously not completely accurate and will tend to under predict the mass of CO_2 by a few percent. However, this will give us a good feel for what to expect for an extreme scenario. The total mass estimated from the model is only 40% of the total injected mass. The contribution of the diffuse volume to gravity is about 17.8 μGal/MT in 1999 and 16.5 μGal/MT in 2001. Assuming a dissolution of 40% (a very large amount) and distributing the missing 20% of the injected mass into patchy saturation volume, the expected gravity change is to 7.4 μGal/yr. For a three year time span, the maximum gravity change would be 22.2 μGal. With less dissolution of CO_2 the change in gravity could be even larger. This signal would be clearly discernable in the gravity data. In fact, assuming no dissolution gives a change of ~13 μGal/yr applying the same logic. Comparing this to the feasibility study of *Williamson et al.* [2001], which predicted 15 μGal/yr for ρ_{co_2} = 350 kg/m^3 and no dissolution, we again see that the detailed flow geometry will have minimal effect on the estimate of CO_2 density from gravity.

To date, no reservoir simulation models have been calculated for temperatures higher than 45 ºC, although heat flow data in the area are consistent with reservoir temperatures of 45 ºC and higher. Therefore, the amount of CO_2 dissolution is speculation at this point. However, it should be clear from the repeat gravity measurements which end of the temperature range the reservoir is in.

The results of this study indicate that time lapse gravimetric reservoir monitoring may play a role in future CO_2 sequestration efforts. This detection technique relies on the density contrast between injected CO_2 and the aquifer fluids, limiting its applicability to fluid filled reservoirs and excluding formations such as depleted coal beds. The best results will be obtained when monitoring shallow reservoirs less than 1000 m deep, where the density of CO_2 is much less than that of the reservoir fluids. In order to halt CO_2 emissions, as is needed to mitigate anthropogenic climate change, hundreds of sites such as Sleipner will be needed along with many other carbon reduction strategies.

Undoubtedly, gravity will be a useful tool for monitoring injected CO_2 for a number of these sites.

Table 1 Summary of the maximum magnitude of the gravity change expected per year for each of the different models. The values given for the seismic horizon models with ρ_{co_2} = 350 kg/m^3 and ρ_{co_2} = 550 kg/m^3 are an estimate of the result of redistributing the diffuse CO_2 to match the pushdown and injected mass (see the text).

Model	**ρ_{CO2} (kg/m^3)**	**Maximum change (μGal/yr)**
Seismic horizon	350	~7.4
Seismic horizon	550	4.5
Seismic horizon	700	2.7
Model I	700	2.2
Model IIa	700	2.4
Model IIb	550	4.7

References

Allis, R.G. and T.M. Hunt, Analysis of exploitation-induced gravity changes at Wairakei geothermal field, *Geophysics*, 51, 1647-1660, 1986.

Arts, R., O. Eiken, A. Chadwick, P. Zweigel, L. van der Meer, and B. Zinszner, Monitoring of CO_2 Injected at Sleipner using time lapse seismic data, in *Abstracts of the 6th International Conference on Greenhous Gas Control Technology (GHGT-6)*, Kyoto, Japan, 2002a.

Arts, R., R. Elsayed, L. van der Meer, O. Eiken, S. Østmo, A. Chadwick, G. Kirby, and B. Zinszner, Estimation of the mass of injected CO_2 at Sleipner using time-lapse seismic data, in *EAGE, Annual meeting*, Florence, Italy, 2002b.

Baklid, A., Korbøl, R. and Owren G.: Sleipner Vest CO_2 disposal, CO_2 injection into a shallow underground aquifer. Paper presented on the 1996 SPE Annual technical Conference and Exhibition, Denver, Colorado, USA, SPE paper 36600, 1-9, 1996.

Chadwick, R.A., R. Arts, and O. Eiken, 4D seismic quantification of a growing CO_2 plume at Sleipner, North Sea, *unpublished*, 2002.

Chadwick, R.A., R. Arts, O. Eiken, G.A. Kirby, E. Lindeberge, and P. Zweigel, 4D seismic imaging of an injected CO_2 plume at the Sleipner Field, central North Sea, in *3D Seismic Technology*, edited by R.J. Davies, J.A. Cartwright, S.A. Stewart, M. Lappin, and J.R. Underhill, Geological Society of London, London, 2004.

Eiken, O., Zumberge, M. and Sasagawa, G., Gravity monitoring of offshore gas reservoirs. Expanded Abstract from SEG Annual Meeting 2000, 2000.

Fialko, Y., Khazan, Y., and Simons, M., Deformation due to a pressurized horizontal circular crack in an elastic half-space, with applications to volcano geodesy, *Geophys. J. Int.*, 146, 181-190, 2001.

Nooner, S., Zumberge, M., Sasagawa, G., Eiken, O., and T. Stenvold, A baseline seafloor gravity Survey over the Sleipner CO_2 sequestration site, *3rd Annual Carbon Capture and Sequestration Proceedings*; ExchangeMonitor Publications; Washington DC; www.carbonsq.com, 2004.

Mavko, G., and T. Mukerji, Bounds on low-frequency seismic velocities in partially saturated rocks, *Geophysics*, *63* (3), 918-924, 1998.

Mogi, K., Relation between the eruptions of various volcanos and the deformation of the ground surfaces around them, *Tokyo Univ. Earthquake Res. Inst. Bull.*, 36, 99-134, 1958.

San Andres, R.B. and J.R. Pederesen, Monitoring the Bulalo geothermal reservoir, Philippines, using precision gravity data, *Geothermics*, 22, 395-402, 1993.

Sasagawa, G.S., Crawford, W., Eiken, O., Nooner, S., Stenvold, T. and Zumberge, M.A., A new sea-floor gravimeter, *Geophysics*, 68, 2, 544-553, 2003.

Williamson, J.O., Chadwick, R.A., Rowley, W.J. and Eiken, O., Gravity modeling of the CO2 bubble. BGS Commisioned Report CR/01/063. *Internal SACS Report*, 2001.